Catalysis Today 139 (2008) 109–112

Contents lists available at ScienceDirect

Catalysis Today

journal homepage: www.elsevier.com/locate/cattod

A comparative study of photocatalytic degradation of phenol of TiO_2 and ZnO in the presence of manganese dioxides

Shunjun Li, Zichuan Ma *, Jie Zhang, Yinsu Wu, Yamin Gong

College of Chemistry and Material Sciences, Hebei Normal University, Shijiazhuang, Hebei 050016, PR China

ARTICLE INFO

Article history:
Available online 11 September 2008

Keywords:
TiO_2
ZnO
MnO_2
Phenol
Deactivation
Photocatalysis

ABSTRACT

The effects of the presence of α-MnO_2, β-MnO_2 and δ-MnO_2 on the photocatalytic degradation of phenol by TiO_2 and ZnO have been investigated. Experiments were conducted in a batch reactor, at initial pH 6.0 and 25 °C. The results showed that the TiO_2-photocatalytic degradation of phenol was inhibited completely in the first 20–60 min in the presence of three crystal types of MnO_2 whereas the ZnO-photocatalytic degradation of phenol only declined slightly. UV-vis diffuse reflectance spectroscopy (DRS) and surface photovoltage spectroscopy (SPS) analysis implied that the interaction of MnO_2 with TiO_2 and ZnO could change the energetic of these two photocatalysts.

1. Introduction

In recent years, numerous studies have been reported on the photocatalytic degradation of organic compounds using semiconductor particles as photocatalysts [1–6]. Among the semiconductors employed, TiO_2 and ZnO are most extensively used photocatalysts in recent years. They are known as inexpensive, nontoxic and very effective semiconductor photocatalysts [4–6]. However, the deactivation of TiO_2 by trace amount of other species present in natural water or wastewater is one of the major problems which prevent the technology from practical application. It is known that some coexisting inorganic ions, such as Cu^{2+}, Mn^{2+}, Ni^{2+}, Co^{2+}, Cr^{3+}, SO_4^{2-}, $H_2PO_4^-$, HCO_3^-, I^-, and $Cr_2O_7^{2-}$, could suppress the photocatalytic activity of TiO_2 in the degradation process of certain pollutants [7–10]. Moreover, Yu et al. reported that some intermediates generated in the photocatalytic degradation of aromatic compounds, such as benzoic acid and hydrobenzoic acid, could deactivate TiO_2 photocatalysts [11]. Colón et al. reported that in the presence of salicylic acid, the significant deactivation of TiO_2 in the TiO_2-photocatalytic reduction of Cr(VI) was observed [12,13]. However, up to now, a few reported investigations on the deactivation of photocatalysts deal mainly with dissolved substrates which are detrimental to the activity of the photocatalysts. In fact, the composition of wastewater is very complex. It contains not only various dissolved species, but also a variety of particulate species (e.g., manganese oxides, iron oxides, and clay minerals) [14]. Nevertheless, to the best of our knowledge, the detrimental influence of particulate species on the activity of photocatalysts has been seldom reported.

In our previous work [15,16], it was found that manganese dioxide was able to markedly inhibit the photocatalytic activity of P25 TiO_2 in the degradation of methyl orange, which is a representative azo dye. However, the influence of MnO_2 on photocatalyst TiO_2 in the degradation of other pollutants, and the effect of MnO_2 on the photocatalytic activity of ZnO, are not known well. Hence, the objective of this research is to (1) study the influence of MnO_2 on TiO_2-photocatalytic degradation of phenolic type pollutants using phenol as a model pollutant, (2) examine the effect of MnO_2 on ZnO-photocatalytic degradation of phenol, and (3) investigate the differences in the interaction of MnO_2 with ZnO and TiO_2 in suspension by DRS and SPS. This study may provide some insight into the design of highly tolerant photocatalysts.

2. Experimental

2.1. Materials and instruments

P25 TiO_2 was purchased from the Degussa Company in Germany, and used as the photocatalyst. It is approximately composed of 80% anatase and 20% rutile, and has a Brunauer–Emmet–Teller (BET) surface area of 50 $m^2\ g^{-1}$, a mean particle size of 30 nm, and a pH_{zpc} of 6.25 [1]. Commercial nanoparticle ZnO (a

* Corresponding author. Tel.: +86 311 86268343; fax: +86 311 86269217.
E-mail address: ma_zichuan@163.com (Z. Ma).

0920-5861/$ – see front matter © 2008 Elsevier B.V. All rights reserved.
doi:10.1016/j.cattod.2008.08.012

mean particle size of 33 nm, Institute of NanKai University, China), was employed as another photocatalyst. Three crystal types of manganese dioxide (α-MnO_2, β-MnO_2, δ-MnO_2) were prepared according to Parida's methods [17]. These obtained MnO_2 were dried at 110 °C, ground, then passed through a 100-mesh sieve. α-MnO_2 comprised rod-like particles with an average diameter of 25 nm and a length of 450 nm; while β-MnO_2 was made up of irregularly shaped particles of average size 200 nm. δ-MnO_2 comprised spherical particles with an average diameter of 250 nm. Phenol employed was commercial analytical reagent (Guangfu Institute of Fine Chemical Research, Tianjin, China). The pH value of the solution was adjusted using aqueous solution of either NaOH or $HClO_4$. A JB-3A magnetic stirrer (Shanghai Precision & Scientfic Instruments Co., Ltd., China) was utilized to make the obtained suspension uniform. The pH value of the solution was measured by a pHS-3B pH meter (Shanghai Precision & Scientfic Instruments Co., Ltd., China). Phenol concentration was analyzed using a VIS-7220 spectrophotometer (Shanghai Precision & Scientfic Instruments Co., Ltd., China) with the method of 4-amino antipyrine at 510 nm [18].

2.2. Evaluation of the photocatalysis

Photocatalyic tests were performed in a cylindrical glass container (with an inner diameter of 55 mm and length of 110 mm) with a cooling jacket to control the reaction temperature. The irradiation source was a high-pressure mercury UV lamp, presenting an intense emission band centred at 365 nm (70 W, Suzhou Fullite Lighting Co., Ltd., China). In the experiment, the distance between the UV lamp and photocatalytic reactor was fixed 100 mm. A total of 100 mL of phenol solution (20 mg L^{-1}) was first introduced into the container and the pH value was adjusted to 6.0. Then, 20 mg of the photocatalysts (200 mg L^{-1}) and 2 mg of MnO_2 (20 mg L^{-1}) were dispersed into the above solution. In the control experiment, no MnO_2 was added. Prior to irradiation, the obtained suspension was stirred at 25 °C in the dark for 90 min, to ensure sufficient contact between MnO_2 and photocatalyst particles, and to achieve the adsorption/desorption equilibrium between phenol and suspended solid particles. After the equilibrating period, an aliquot of solution was taken from the reactor to measure the phenol concentration. The concentration measured was used as the initial concentration (C_0, mg L^{-1}) in the treatment of reaction kinetic data. During the photocatalytic reaction, a 5-mL reaction suspension was withdrawn from the reactor at a given time interval. The obtained suspension was filtered through a 0.22-μm millipore filter, the phenol concentration (C, mg L^{-1}) in the filtrate was quantified by using the spectrophotometer. The reported degradation percentage (η) of phenol was the percentage of phenol consumed ($\eta = [(C_0 - C)/C_0] \times 100$). The influences of MnO_2 on the photocatalytic activity of TiO_2 and ZnO were evaluated based on the change in kinetic curve.

2.3. Characterization of photocatalysts

Prior to characterization, TiO_2, ZnO, MnO_2, MnO_2-contaminated TiO_2 and ZnO were dried. SPS measurement of the samples was carried out with a home-built apparatus that has been described in references [19,20]. It was performed by a photovoltage cell, mainly consisting of two ITO quartz glass electrodes. The difference between the surface potential barrier in the light and the one in the dark is the SPS signal.

UV–vis DRS was acquired on a Hitachi U-3010 spectrophotometer with an integrating sphere (model 130-0632). The spectra were measured in the range 200–600 nm, with $BaSO_4$ used as reference.

3. Results and discussion

3.1. Effect of MnO_2 on the TiO_2-photocatalytic degradation of phenol

Three crystal types of manganese dioxide, i.e., α-MnO_2, β-MnO_2 and δ-MnO_2, which exist widely in the environment [21], were used in this experiment. To examine the effects of manganese dioxides on the TiO_2-photocatalytic degradation of phenol, the three crystal types of MnO_2 were dispersed into the TiO_2/phenol system. They were denoted as TiO_2/α-MnO_2, TiO_2/β-MnO_2, and TiO_2/δ-MnO_2 respectively.

Fig. 1 shows the kinetic curves of phenol photocatalytic degradation on P25 TiO_2 photocatalyst and MnO_2-contaminated TiO_2 photocatalysts (TiO_2/α-MnO_2, TiO_2/β-MnO_2, and TiO_2/δ-MnO_2). Under the same condition, the three crystal types of pure MnO_2 presented no photocatalytic activity (the results were not shown here). From Fig. 1, it can be seen that the degradation percentage of phenol was more than 90% in 150 min of irradiation when pure TiO_2 was used as the photocatalyst. However, the presence of MnO_2 significantly altered the degradation percentage of phenol. In the presence of α-MnO_2 and δ-MnO_2, the concentration of phenol dropped to a constant value during the first 20 min. When β-MnO_2 was added, a similar phenomenon was observed at the first 60 min. The results illustrate that the presence of MnO_2, even in a trace amount, can inhibit the photocatalytic activity of TiO_2 significantly, and in some cases, deactivate the photocatalyst completely. Moreover, under the same conditions, for different crystalline MnO_2, the inhibitory effects are various and the poisoning effect is in the order of δ-MnO_2 > α-MnO_2 > β-MnO_2. The observations are in accordance with that of TiO_2-photocatalytic degradation of methyl orange in the presence of MnO_2 [15]. Therefore, the poisoning effect of MnO_2 will occur during the TiO_2-photocatalytic degradation of both azo dye and phenolic compounds.

3.2. Effect of MnO_2 on the ZnO-photocatalytic degradation of phenol

The photocatalysis experiments of ZnO were also carried out in the same way as stated in Section 3.1. The kinetic curves of phenol photocatalytic degradation over ZnO in the absence and presence of MnO_2 (ZnO, ZnO/α-MnO_2, ZnO/β-MnO_2, and ZnO/δ-MnO_2) were examined, and the results are shown in Fig. 2. As can be seen, the ZnO-photocatalytic degradation of phenol only declined slightly in the presence of MnO_2, which means that MnO_2 cannot deactivate ZnO photocatalyst. By comparison, the decline of ZnO photocatalytic activity caused by the presence of different crystalline MnO_2 is in the order of δ-MnO_2 > α-MnO_2 > β-MnO_2. This is same

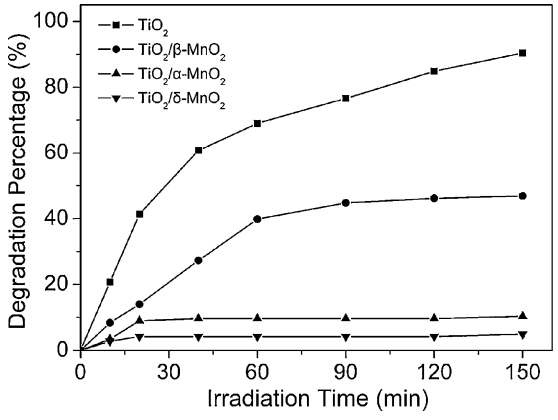

Fig. 1. Changes of degradation percentage of phenol with time (20 mg L^{-1} phenol, initial pH of 6.0, 70 W of UVA, 200 mg L^{-1} of TiO_2, 20 mg L^{-1} of MnO_2, 25 °C).

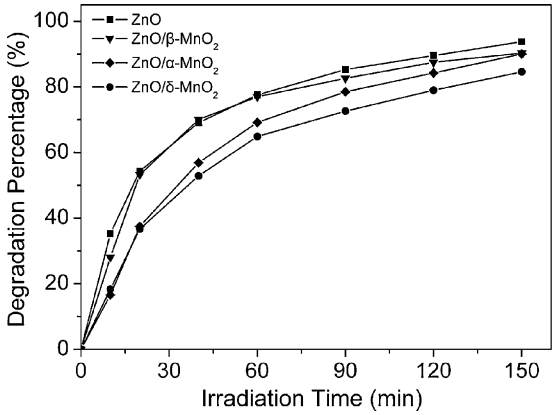

Fig. 2. Changes of degradation percentage of phenol with time (20 mg L^{-1} phenol, initial pH of 6.0, 70 W of UVA, 200 mg L^{-1} of ZnO, 20 mg L^{-1} of MnO_2, 25 °C).

as that of TiO_2 photocatalyst, but the effect of degree is quite different.

Based on the above results, it can be concluded that the TiO_2 photocatalyst is susceptible to MnO_2 poisoning, while photocatalyst ZnO can resist MnO_2 poisoning. This finding may have significant implications for the design of a highly tolerant photocatalyst.

3.3. Measurements of DRS

It is well known that the optical absorption behavior of photocatalyst significantly affects the photocatalytic activity of the photocatalyst. In general, the red-shift in the absorption band edge and the increase in absorption intensity enhance photocatalytic activity due to the enhanced formation of photoelectrons and photoholes [22–24]. The opposite is also true. To find out why MnO_2 has such a different effect on the activity of the two photocatalysts, the interactions of MnO_2 with both photocatalysts were studied by UV–vis DRS.

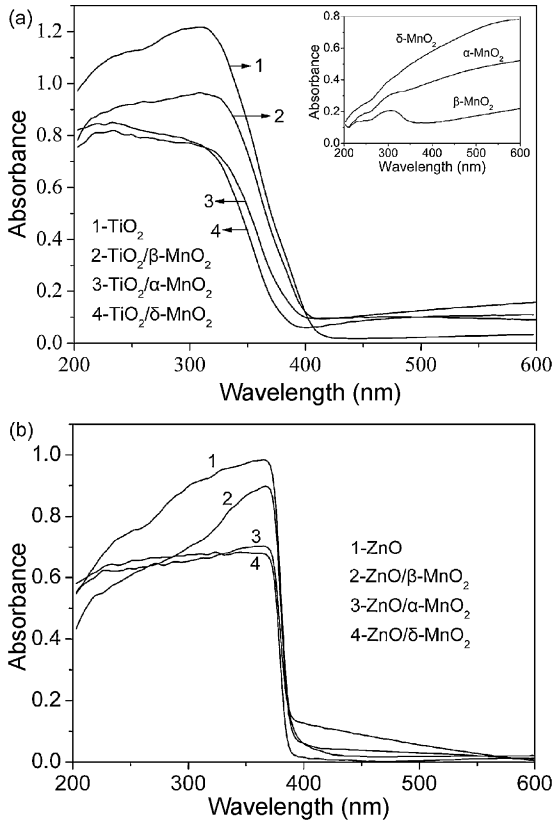

Fig. 3. DRS of TiO_2 (a) and ZnO (b) before and after contaminated, inset of (a) showing DRS of three types of MnO_2.

Inset of Fig. 3(a) shows the DRS of an equivalent amount of different crystalline MnO_2. As shown in the inset, the optical absorption intensity of different crystal types MnO_2 steadily increase from 200 nm to 600 nm, and no clear band edge is observed. The results indicate that MnO_2 is not a typical semiconductor. The DRS of pure TiO_2 and MnO_2 incorporating TiO_2 are shown in Fig. 3(a). The spectra of the latter were obtained by subtracting the absorption of equivalent MnO_2 from spectra of the mixture [15], which should reflect the changes in absorption of TiO_2 in the mixture of MnO_2 and TiO_2. Due to the presence of MnO_2, the absorption spectra of TiO_2 vary substantially. It is noted that the absorption band edge is blue-shifted and the absorption intensity is decreased. The decrease in the photocatalytic activity of TiO_2 in the presence of MnO_2 clearly results from the decline in the formation of photoelectron and photoholes due to the lower absorption of UV photons and the change in band energetics. The order of the effect on TiO_2 absorption by different MnO_2 is δ-MnO_2 > α-MnO_2 > β-MnO_2, which matches the order of their poisoning effect. For comparison, the DRS of ZnO was also measured and presented in a similar way as shown in Fig. 3(b). Unlike the TiO_2 spectra, the presence of MnO_2 only caused ZnO UV absorption intensity to decrease, and its absorption band edge remained unchanged. This implies that the presence of MnO_2 does not change the band energetics of ZnO. The order of the effect on ZnO UV absorption by different crystalline MnO_2 is δ-MnO_2 > α-MnO_2 > β-MnO_2, which matches the order of their declining effect on ZnO-photocatalytic degradation of phenol. The different changes in the band edge of the two photocatalysts caused by MnO_2 may reflect the difference in the interaction of the two photocatalysts with MnO_2.

3.4. SPS analysis

To further elucidate the mechanism, surface photovoltaic properties of the two photocatalysts in the presence and absence of MnO_2 have been studied by SPS. Based on the peak position, the response range, and the intensity of SPS, it can offer important information about the distribution of energy levels of conduction band and surface state, as well as the separation and recombination behavior of the photoinduced electron–hole pairs. It is well known that the higher the SPS signal, the higher the separation rate of photoinduced charge carriers [25,26]. Fig. 4(a) shows SPS responses of TiO_2 and TiO_2/α-MnO_2 (α-MnO_2 alone has no photovoltage signal). As shown in the spectra, the threshold wavelength of the TiO_2 response is shifted from 410 nm to 370 nm, and the intensity is decreased markedly, when it is contaminated by α-MnO_2. This suggests that the band gap of TiO_2 is broadened by MnO_2, which is in agreement with the results of DRS. Possibly MnO_2 can also accelerate the recombination of photoinduced electron–hole pairs via some impurity subbands. These effects lead to the deactivation of the photocatalytic activity of TiO_2.

Shown in Fig. 4(b) are the SPS responses of ZnO and ZnO/α-MnO_2. The presence of MnO_2 also blue-shifts the threshold wavelength response of ZnO from 420 nm to 405 nm. In comparing their absorption band edges, we found that the SPS threshold wavelength of ZnO is longer than the absorption band edge of ZnO, and the surface voltage generated at the longer wavelength than its absorption band edge may originate from the subbands of surface states of ZnO. In general, the photoinduced electrons can be trapped by the surface states and then transfered to the adsorbed

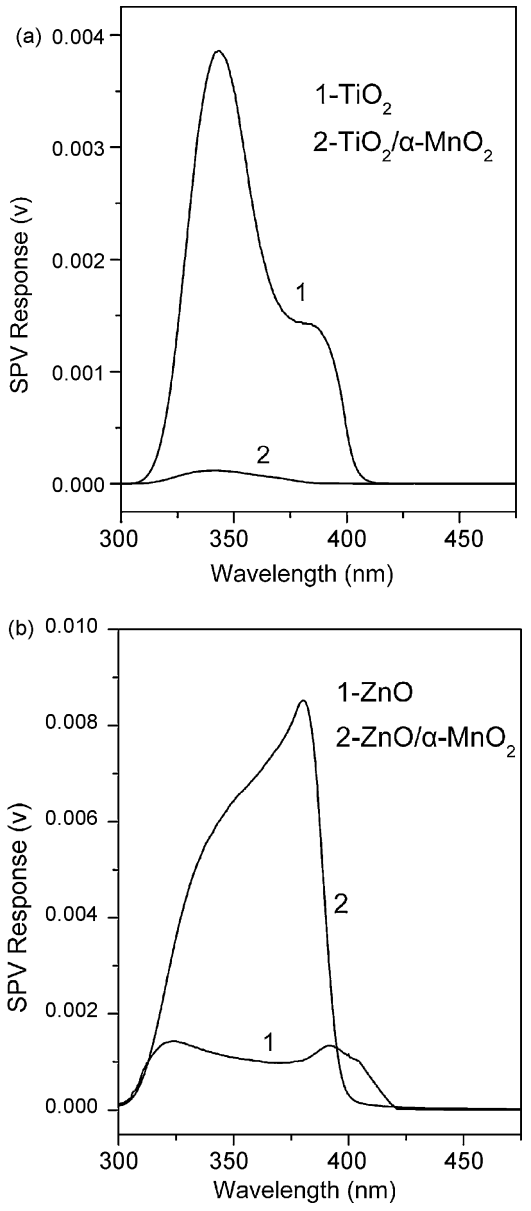

Fig. 4. SPS of TiO_2 (a) and ZnO (b) before and after contaminated.

O_2 on the photocatalyst to produce superoxide radical ion ($\bullet O_2^-$) during the process of photocatalytic reaction [26]. The interaction of MnO_2 with ZnO may eliminate such surface states as evidenced by alignment of SPS threshold and the absorption band edge of ZnO when MnO_2 is present. Therefore, this certainly will suppress the photoelectron trapping via the surface state subbands and decrease the formation rate of superoxide anion, which is unfavourable to the photocatalytic activity. However, in contrast, at wavelength shorter than absorption band edge, the increase in surface voltage of ZnO caused by the presence of MnO_2 is observed, indicating that the ZnO/α-MnO_2 sample has high separation rate of photoexcited carriers. This effect should have increased the photocatalytic activity of ZnO. Hence, the collective result is that the photocatalytic activity of ZnO remains relatively unchanged.

4. Conclusions

The present work has shown that the TiO_2-photocatalytic degradation of phenol can be significantly inhibited in the presence of α-MnO_2, β-MnO_2 or δ-MnO_2, but its inhibitory effect on the ZnO-photocatalytic degradation of phenol is negligible. The poisoning effect for TiO_2 by three crystal types of MnO_2 under the same conditions is in the order δ-MnO_2 > α-MnO_2 > β-MnO_2. The characterizations indicate that the interaction of MnO_2 with TiO_2 and ZnO could change the energetics of these two photocatalysts. The interaction of MnO_2 with ZnO eliminates its surface state subbands, while such interaction with TiO_2 creates more impurity subbands leading to the accelerated photoelectron and photohole recombination.

Acknowledgements

This work was supported by the National Natural Science Foundation of China (No. 20477009) and the Natural Science Foundation of Hebei Province of China (No. E2005000183).

References

[1] M.R. Hoffmann, S.T. Martin, W. Choi, D.W. Bahnemann, Chem. Rev. 95 (1995) 69.
[2] W. Zhao, W.H. Ma, C.C. Chen, J.C. Zhao, Z.G. Shuai, J. Am. Chem. Soc. 126 (2004) 4782.
[3] T. Matsumoto, N. Iyi, Y. Kaneko, K. Kitamura, S. Ishihara, Y. Takasu, Y. Murakami, Catal. Today 120 (2007) 226.
[4] R. Nakamura, A. Imanishi, K. Murakoshi, Y. Nakato, J. Am. Chem. Soc. 125 (2003) 7443.
[5] G. Yu, Z. Chen, Z. Zhang, P. Zhang, Z. Jiang, Catal. Today 90 (2004) 305.
[6] M.M. Uddin, M.A. Hasnat, A.J. Samed, R.K. Majumdar, Dyes Pigment 75 (2007) 207.
[7] C. Chen, W. Ma, J. Zhao, J. Phys. Chem. B 106 (2002) 318.
[8] V. Brezová, A. Blažková, E. Borošvá, M. Čeppan, R. Fiala, J. Mol. Catal. A: Chem. 98 (1995) 109.
[9] R.A. Burns, J.C. Crittenden, D.W. Hand, V.H. Selzer, L.L. Sutter, S.R. Salman, J. Environ. Eng. 125 (2006) 77.
[10] Y.C. Tang, C. Hu, Y.Z. Wang, J. Environ. Sci. 23 (2003) 503.
[11] X.J. Yu, Y.Q. Wang, C.L. Li, S.M. Bai, D.Z. Sun, J. Environ. Sci. 26 (2006) 433.
[12] G. Colón, M.C. Hidalgo, J.A. Navío, J. Photochem. Photobiol. A 138 (2001) 79.
[13] G. Colón, M.C. Hidalgo, J.A. Navío, Langmuir 17 (2001) 7174.
[14] R.A. Petrie, P.R. Grossl, R.C. Sims, Environ. Sci. Technol. 36 (2002) 3744.
[15] S.J. Li, Z.C. Ma, L. Wang, J.Z. Liu, Sci. China. Ser. B 37 (2007) 483.
[16] S.J. Li, Z.C. Ma, K.Q. Ding, J.Z. Liu, Chem. J. Chin. Univ. 28 (2007) 2338.
[17] K.M. Parida, S.B. Kanungo, B.R. Sant, Electrichim. Acta 26 (1981) 435.
[18] F.S. Wei, Water and Exhausted Water Monitoring Analysis Method, China Environmental Science Press, Beijing, 1989, p. 408.
[19] L.Q. Jing, X.J. Sun, J. Shang, W.M. Cai, Z.L. Xu, Y.G. Du, H.G. Fu, Sol. Energy Mater. Sol. Cell 79 (2003) 133.
[20] L.Q. Jing, B.F. Xin, F.L. Yuan, B.Q. Wang, K.Y. Shi, W.M. Cai, H.G. Fu, Appl. Catal. A: Gen. 275 (2004) 49.
[21] D.M. Sherman, Geochim. Cosmochim. Acta 69 (2005) 3249.
[22] R. Asahi, T. Morikawa, T. Ohwaki, Science 293 (2001) 269.
[23] R.J. Tayade, R.G. Kulkarni, R.V. Jasra, Ind. Eng. Chem. Res. 45 (2006) 922.
[24] C. Wang, B.Q. Xu, X. Wang, J. Zhao, J. Solid State Chem. 178 (2005) 3500.
[25] T.F. Xie, D.J. Wang, L.J. Zhu, T.J. Li, Y.J. Xu, Mater. Chem. Phys. 70 (2001) 103.
[26] L.Q. Jing, H.G. Fu, B.Q. Wang, D.J. Wang, B.F. Xin, S.D. Li, J.H. Sun, Appl. Catal. B: Environ. 62 (2006) 282.